JOURNAL OF Applied Polymer SCIENCE

Influence of the Reaction Temperature on Polyaniline Morphology and Evaluation of their Performance as Supercapacitor Electrode

Hao Kuang, Qi Cao, Xianyou Wang, Bo Jing, Qiang Wang, Ling Zhou

Key Laboratory of Environmentally Friendly Chemistry and Applications of Minister of Education, College of Chemistry, Xiangtan University, Xiangtan 411105, China

Correspondence to: Q. Cao (E-mail: wjcaoqi@163.com)

ABSTRACT: The polyaniline (PANI) nanostructures of tubular, spherical, and granules morphologies were synthesized by chemical oxidation approach in different reaction temperatures and used as the active electrode materials of symmetric redox supercapacitors. X-ray diffraction and scanning electron microscopy techniques are employed for characterization of these PANIs. With the initial and reaction temperature increase, the morphology of PANI turned from block to spherical and tubular. Electrochemical properties of these PANI electrodes are studied by cyclic voltammetry (CV), agalvanostatic charge–discharge test, and electrochemical impedance spectroscopy (EIS) in 1*M* H_2SO_4 aqueous solution. The highest electrochemical properties are obtained on the PANI with tubular morphology. The initial specific capacitance of tubular, spherical, and granules PANI are about 300, 300, and 290 F g^{-1} at a constant current of 5 mA. Meanwhile, the retention of the tubular PANI capacitance after 500 charge–discharge cycles was 75%, whereas the spherical and granules PANI was only 35% and 57%. The results indicate that tubular PANI electrodes have potential applications as high-performance supercapacitors electrode materials. © 2013 Wiley Periodicals, Inc. J. Appl. Polym. Sci. 130: 3753–3758, 2013

KEYWORDS: structure–property relations; properties and characterization; batteries and fuel cells; conducting polymers

Received 28 March 2013; accepted 8 June 2013; Published online 29 June 2013

DOI: 10.1002/app.39650

INTRODUCTION

In recent years, supercapacitors have attracted significant attentions in energy storage devices because of their high power density, high energy density, and long cycle life.[1–5] They are applied to various electronic devices, such as power electronics, as well as in hybrid electric vehicles and space flight technology.[1] Supercapacitors can be divided into two types according to the charge–storage mechanism: one is electrical double layer capacitors (EDLCs), which are based on carbon materials and the capacitance arises from the charge separation at an electrode/electrolyte interface; the other is the pseudocapacitors, which are based on conducting polymers/metallic oxide and the capacitance comes from Faradic reactions of the electrode materials.[2,3] The specific capacitance of EDLCs is limited by their effective surface areas but carbon materials can obtain a long cycle life ($>10^5$ cycles).[5,6] Compared with EDLC, pseudocapacitors have much higher specific capacitance because of their redox properties.

Conducting polymers can be positively or negatively charged with ion insertion in the polymer matrix to balance the injected charge, and hence produce the pseudocapacitance.[7] Conducting polymers have been considered as promising candidates among pseudocapacitor electrode materials because of their low cost, low environmental impact, facile synthesis, high conductivity in a doped state, and high pseudocapacitance.[8–12] Besides, conducting polymers offer the advantages of low production cost compared with noble metal oxides and high charge capacity compared with activated carbons.

The common electrical conducting polymers in supercapacitor applications are polyaniline (PANI),[13–18] polypyrrol,[19–21] polythiophene, [21,22] and their corresponding derivatives. Among them, PANI is unique because of its simple nonredox doping/de-doping chemistry based on acid/base reactions.

So far, the nanostructures of PANI have attracted intensive interest because the polymer morphology strongly affects the performance of a supercapacitor, the reason is that it influences the specific surface area of the polymer and ion diffusivity in the polymer matrix during redox switching leading to high specific capacitance.[23] Wang et al.[24] reported a large array of vertically aligned PANI nanowires which obtained a specific capacitance value of 950 F g^{-1} at a current density of 1 A g^{-1}. Zheng et al.[25] obtained a flocculent PANI/carbon nanotubes composite and its capacitance is as high as 837.6 F g^{-1} measured by cyclic voltammetry (CV) at 1 mV s^{-1}.

However, the relationship between the capacitance of PANI electrodes and the reaction temperature is still rarely reported, especially with chemical synthesis method. Herein, we fabricate different morphologies nanostructured PANI materials by

changing the reaction temperatures to study the influence of reaction temperature on the performance of conducting PANI supercapacitors. The electrochemical performances of the PANI supercapacitor are characterized by CV, agalvanostatic charge–discharge test, and electrochemical impedance spectroscopy (EIS) in 1*M* H_2SO_4 electrolyte.

EXPERIMENTAL

Materials

Aniline (ANI, analytical purity, Beijing Chemical Reagent, China) was distilled under reduced pressure and stored refrigerated before use. Salicylic acid (SA), ethanol, and ammonium persulfate (APS) were of analytical grade and used without further treatment. All solutions were prepared with deionized water.

Synthesis of PANI. PANI of three different morphologies were synthesized by chemical oxidative polymerization of aniline in 1*M* SA solution using APS as oxidant (molar ratio of monomers to oxidant = 1:1), and SA as dopant.

Synthesis of Granules Morphology PANI. A solution containing appropriate amount of 1*M* SA was prepared by dissolving a certain amount of SA in deionized water with magnetic stirring till the SA was completely soluble, then a certain amount of ANI was added to the above solution and stirred for an hour. Upon constant stirring, the precooled solution of APS in distilled water was then added drop to the solution at 0–5°C for half an hour. The reaction was then allowed to proceed with agitation for 24 h in the ice–water bath. Finally, the products were obtained by filtration and washing with ethanol and distilled water, until the filtrate became colorless, and then dried under vacuum at 60°C for 48 h.

Synthesis of Tubular Morphology PANI. A solution containing appropriate amount of 1*M* SA was prepared by dissolving a certain amount of SA in deionized water with magnetic stirring till the SA was completely soluble, then a certain amount of ANI was added to the above solution and stirred for an hour. Upon constant stirring, the solution of APS in distilled water was then added dropwise to the solution at room temperature immediately. The reaction was then allowed to proceed with agitation for 24 h at room temperature. Finally, the products were obtained by filtration and washing with ethanol and distilled water, until the filtrate became colorless, and then dried under vacuum at 60°C for 48 h.

Synthesis of Spherical Morphology PANI. A solution containing appropriate amount of 1*M* SA was prepared by dissolving a certain amount of SA in deionized water with magnetic stirring till the SA was completely soluble, then a certain amount of ANI was added to above solution and sonicated for an hour. Upon constant stirring, the solution of APS in distilled water was then added dropwise to the solution at room temperature immediately. The reaction was then allowed to proceed with agitation for 24 h in the ice–water bath. Finally, the products were obtained by filtration and washing with ethanol and distilled water, until the filtrate became colorless, and then dried under vacuum at 60°C for 48 h.

Characterization of the Materials

The morphologies of the electrodes were examined by means of scanning electron microscopy (SEM) (Hitachi S-3500N, Japan). The X-ray diffraction (XRD) patterns of the obtained samples were characterized by using a Rigaku/DMAX 2400 diffractometer (Japan) with CuKα radiation ($\lambda = 1.54178$ Å) monochromated radiation operating at 40.0 kV and 60.0 mA. XRD data were collected in the 2θ ranging from 3° to 90°.

Electrochemical Measurements

In the experiment, all electrochemical properties of PANI samples were performed in 1*M* H_2SO_4 using a symmetrical sandwich-type two-electrode capacitor cell at room temperature. The slurry was prepared by mixing the PANI samples with polyvinylidenefluoride and acetylene black in N-methyl-2-pyrrolidone at the mass ratio of 80:10:10, and stirred the mixture sufficiently at room temperature. After that, the homogenous slurry was pressed onto a steel mesh with a size of 1 cm^2 (the steel mesh functions as current collector), yielding working electrodes with the total active mass of 4–8 mg. Before testing, the electrodes were dried at 60°C for 12 h in vacuum then weighed. Sandwich-type supercapacitor, consisted of two electrodes with similar mass and a piece of separator, was assembled. The capacitive behaviors were measured by means of Potentiodynamic CV (1, 2, 5, 10 mV s^{-1}) and EIS (10^{-2}–10^5 Hz, amplitude of signal 5 mV) measurement were conducted in an electrochemical workstation (Zahner Im6ex). The capacitance behaviors of PANI electrodes were evaluated by galvanostatic charge/discharge cycling in the potential range between 0 and 0.8 V at the same current density (5 mA) using a Neware battery testing system (BTS-XWJ-6.9.27s) multichannel generator, as well as multicycle charge/discharge at a current density of 5 mA.

The specific capacitance of the electrode is obtained from the following equation:

$$C = {}^{2}i\Delta t/_{M}\Delta V \quad (1)$$

where C is the single electrode capacitance (F g^{-1}), i is the constant discharge current density (A), Δt the discharging time (s), M is the mass of the single active electrode material, and ΔV is the potential change apart from the ohmic drop.

RESULTS AND DISCUSSION

Structural Characteristics

Figure 1 shows SEM images of different morphologies of PANI. Figure 1(a–c) is corresponding to granules, spherical, and tubular, respectively. As shown in Figure 1(a), SEM image of PANI exhibits a granules structure with particle diameter about 100 nm. It can be observed that the morphology of PANI has been changed from Figure 1(b), which exhibits an uneven spherical structure. Figure 1(c) exhibits a tubular structure with grain diameter is about 200 nm. From Figure 1, it can be concluded that the morphology of PANI was greatly influenced by the reaction temperatures. The solution was mixed at low temperature and then reaction in the ice–water bath, we could get granules morphology PANI. But mixed solution at room temperature and then reaction in the ice–water bath, the morphology of PANI was spherical. Meanwhile, mix the solution at room temperature and then reaction at room temperature, the morphology of PANI became tubular. The results may be

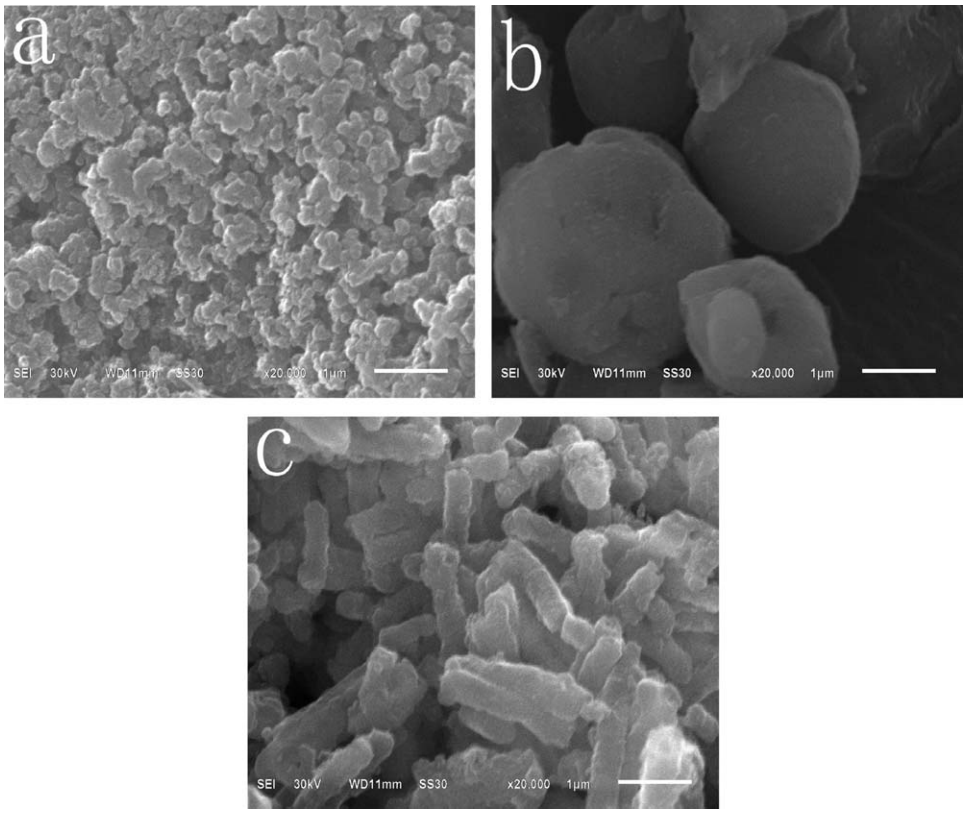

Figure 1. SEM images of PANI nanostructures with: (a) granules, (b) spherical, and (c) tubular morphologies.

because of these soft template formed by SA were not in the same shape in different temperatures. High temperature formed spherical soft templates, low temperatures formed granules soft templates. The reaction at room temperature helped to form granules soft templates. PANI structure characteristics make electrolyte can fully assault embellish electrode active substances, which are helpful for the electrolyte ions moving fast, so as to increase the electrode utilization of active material, resulting in good electrochemical performance.

Figure 2 shows the XRD pattern of the PANI nanostructures with tubular, spherical, and granules morphologies. The three main diffraction peaks of the crystalline PANI are measured to be $2\theta = 6.4°$ ($d = 13.8$ Å), $18.5°$ ($d = 4.79$ Å), $26.0°$ ($d = 3.4$ Å), which are all the characteristic peaks of the PANI. The strong, narrow peak centered at $2\theta = 18.5°$ is ascribed to the periodicity in the direction parallel to the polymer chain, whereas the peak at $2\theta = 26.0°$ is because of the periodicity in the direction perpendicular to the polymer chain.[26] The peak at around $2\theta = 6.0°$ is only observed for highly ordered PANI in which PANI chain distance increases by effective interdigitations of dopant molecules.[27] The increase in the peak intensity at $2\theta = 6.0°$ indicates that the SA-doped PANI ordering in the molecular chains increases with increase in the micronsized fibers length.[27] As we see in Figure 2, the granules morphology PANI with the peak centered at $2\theta = 26.0°$ has split into two small peak, which may be because of the small nanoparticle size and nonuniform distribution.

Electrochemical Characterization

Figure 3 shows CV of PANI supercapacitors in the $1M$ H_2SO_4 aqueous electrolytes with different morphologies of granules (a), spherical (b), tubular (c), and all of them at 1 mV s^{-1} scan rates (d). In Figure 3, PANI electrodes display relatively rectangular voltammograms when the scan rates increase from 1 to 10 mV s^{-1} meaning good capacitive behavior. In addition, with the scanning speed increase, the peak current also linearly increases accordingly, this suggests that tubular PANI electrode

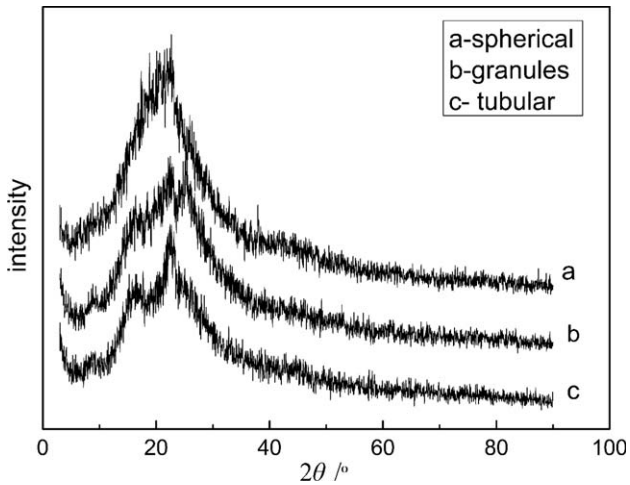

Figure 2. XRD patterns of PANI nanostructures with: (a) granules, (b) spherical, and (c) tubular morphologies.

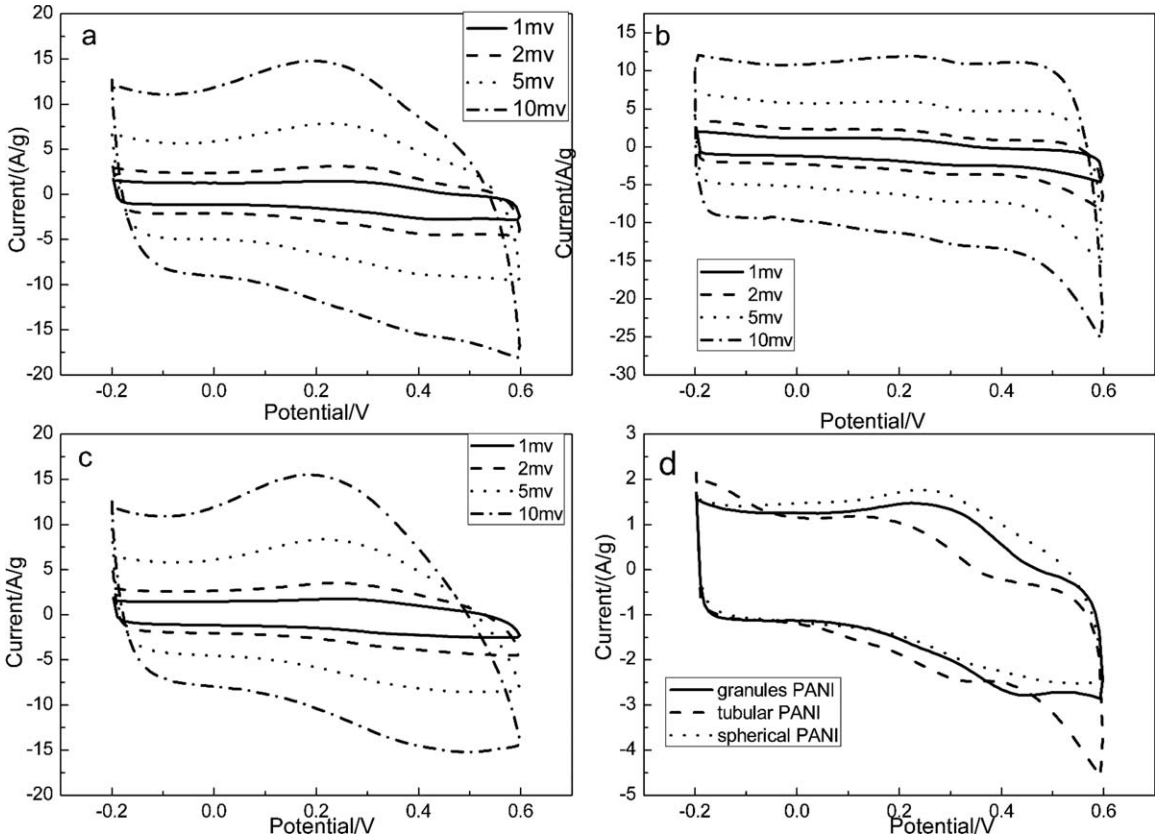

Figure 3. CV of PANI supercapacitors in the 1*M* H_2SO_4 aqueous electrolytes with different morphologies of (a) granules, (b) tubular, (c) spherical, and (d) all of them at 1 mV s^{-1}.

material has good rate characteristics. Disappointed, the voltammograms of spherical PANI supercapacitors [Figure 3(c)] do not show ideal behavior with a rectangular CV shape. In Figure 3(d), it is clear that all morphologies PANI electrodes capacitance characteristics are different from double layer capacitors. CV curves are not the ideal rectangular characteristics, but appeared as two oxidation–reduction peaks. The two oxidation–reduction peaks are corresponding to the conversion of the reduction state PANI and oxidation state PANI reaction, this is pseudocapacitance.

High electrochemical stability can be characterized by galvanostatic charge/discharge. Figure 4 presents the charge/discharge curves of the different morphologies PANI supercapacitors measured at the current densities of 5 mA in 1*M* H_2SO_4 electrolyte (between 0 and 0.8 V). At the beginning of discharge there are a few sudden potential drop (IR drop) that are attributed to the resistance of electrolytes and the inner resistance of ion diffusion in micropore. Usually, IR drop is a direct measure of equivalent series resistance (ESR), which influences the overall power performance of a capacitor. The inset in Figure 4 depicts the IR drop of tubular PANI (a) and granules PANI (b) supercapacitors that can clearly calculate the IR value. It can be found that the IR drop for the tubular PANI supercapacitors is smaller than granules PANI. PANI(c) is not isosceles triangle, and the charging time is very long so we can find that spherical PANI will not show good cycle stability. According to eq. (1), the specific capacitance of the tubular PANI electrode, the granules PANI electrode, the spherical PANI electrode are 300, 290, and 300 F g^{-1}, respectively. The results can be clearly seen that the specific capacitance of PANI has a little change with different reaction temperatures.

Long cycle life of supercapacitors is paramount evaluation for practical applications. Figure 5 reveals the change of specific capacitance versus cycle number for different morphologies PANI supercapacitors in the aqueous electrolytes of 1*M* H_2SO_4

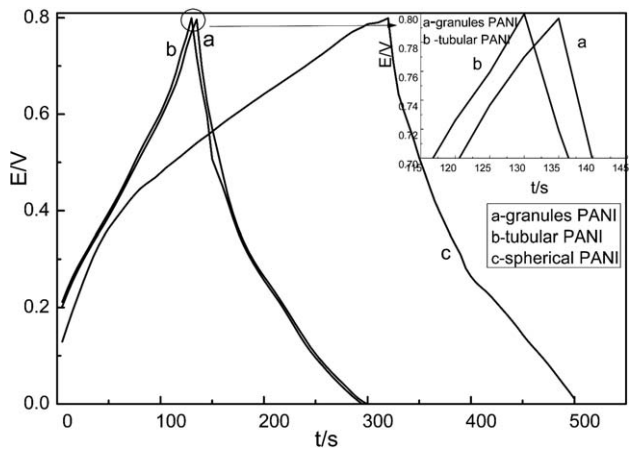

Figure 4. The agalvanostatic charging–discharging curves of the different morphologies PANI supercapacitors at the current densities of 5 mA in 1*M* H_2SO_4.

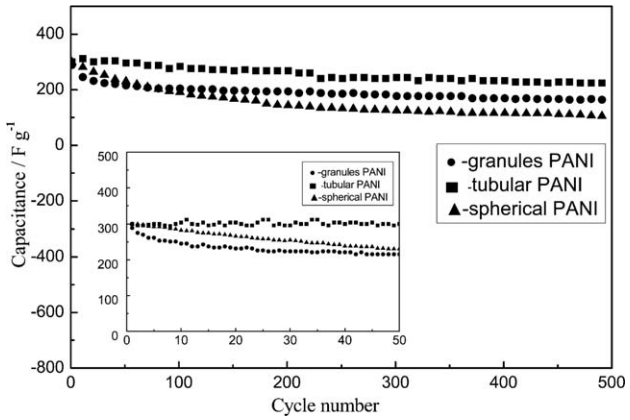

Figure 5. The cycle life curve of the different morphologies PANI supercapacitors in the aqueous electrolytes of 1*M* H_2SO_4 at the current density of 5 mA.

at a current density of 5 mA. At the first cycle, the specific capacitance of the tubular PANI electrode, the granules PANI electrode, and the spherical PANI electrode are 300, 290, and 300 F g^{-1}, respectively. After 1000 consecutive cycles, the specific capacitances keep still at 224, 164, and 105 F g^{-1}, respectively. In addition, the initial capacitance only fades 25%, 43%, and 65%, respectively. The results indicate that the tubular PANI cycle stability is the best of them. Disappointed, the cycle life curve of spherical PANI supercapacitors does not show ideal behavior of the cycle life curve, this is also consistent with the result of the galvanostatic charge/discharge. Besides, this is also consistent with the cycle life curve results in the cycle curves of the different morphologies PANI supercapacitors at the beginning cycles (Figure 5 insert). So the tubular PANI material is expected to become a super capacitor electrode material.

Figure 6 is the Nyquist curve of three different morphologies PANI electrodes in the same potential, with the frequency ranging from 10^5 to 10^{-2} Hz. EIS was measured to analyze the electrochemical properties of supercapacitors about characteristic frequency responses. As Figure 6 shows, the plot features

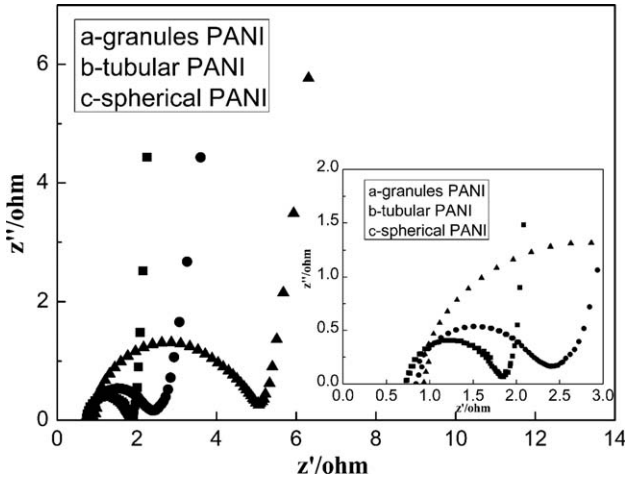

Figure 6. Nyquist plot based on the different morphologies PANI electrodes with the frequency range of 10^5-10^{-2} Hz.

two distinct traits: a high-frequency semicircle and a low frequency spike. In the range of high frequency, the intercept of the semicircle with the real axis represents ESR, including the resistance of the electrolyte solution, the intrinsic resistance of activation material, and the contact resistance of the interface active material/current collector.[28] Here, it can be seen that the three impedance curves of ohms resistor are similar, this is because of the size of the ohm resistor and the electrolytes but has nothing to do with the morphology of PANI. The ESR value of tubular PANI, spherical PANI, and granules PANI are about 0.4, 1.9, and 0.6 Ω, respectively. This is also proved that the tubular PANI electrode that has more superior electric property. We can also find that this tubular PANI in the low frequency line is the straightest of all three Nyquist curve, which means that this tubular PANI electrode has a good capacitive behavior.

CONCLUSION

In this article, we use the chemical oxidation polymerization methods for the synthesis of tubular PANI, spherical PANI, and granules PANI materials with different reaction temperatures. SEM, XRD, CV, circle life, exchange impedance test methods were characterized for the PANI materials. The results show that the morphology of PANI was greatly influenced by the reaction temperatures. The specific capacitance of these samples is similar but the cycle performance of materials is significantly different. Compared with other samples, the tubular morphology PANI exhibits best capacitive performance and has high specific capacitance of 300 F g^{-1} at a constant current of 5 mA. Meanwhile, the retention of the tubular PANI capacitance after 500 charge–discharge cycles was 75%. The results of electrochemical measurements show that tubular PANI electrodes have a potential application as supercapacitor electrode.

ACKNOWLEDGMENTS

The authors gratefully appreciate the supports from the Youth Project of National Nature Science Foundation of China (Grant No. 51103124 and Grant No. 51203131) and Hunan province universities innovation platform of Open Fund Project (11K067).

REFERENCES

1. Burke, A. *J. Power Sources* **2000**, *91*, 37.
2. Conway, B. E. Electrochemical Supercapacitors; Kluwer Academic: New York, **1999**.
3. Conway, B. E. *J. Electrochem. Soc.* **1991**, *138*, 1539.
4. Xue, T.; Xu, C. L.; Zhao, D. D.; Li, X. H.; Li, H. L. *J. Power Sources* **2007**, *164*, 953.
5. Largeot, C.; Portet, C.; Chmiola, J.; Taberna, P.; Gogotsi, Y.; Simon, P. *J. Am. Chem. Soc.* **2008**, *130*, 2730.
6. He, X. J.; Geng, Y. J.;Qiu, J. S.; Zheng, M. D.; Long, S.; Zhang, X. Y. *Carbon* **2010**, *48*, 1662.
7. Zhou, H. H.; Chen, H.; Luo, S. L. *J. Solid State Electrochem.* **2005**, *9*, 574.
8. Lota, G.; Tyczkowskib, J.; Kapicab, R.; Lotac, K.; Frackowiaka, E. *J. Power Sources* **2010**, *195*, 7535.

9. Prasad, K. R.; Kogaand, K.; Miura, N. *Chem. Mater.* **2004**, *16*, 1845.
10. Zhou, Y; He, B.; Zhou, W.; Huang, J.; Li, X.; Wu, B.; Li, H. *Electrochim. Acta* **2004**, *49*, 257.
11. Gupta, V.; Miura, N. *Mater. Lett.* **2006**, *60*, 1466.
12. Fan, L.; Maier, J. *Electrochem. Commun.* **2006**, *8*, 937.
13. Kim, K. S.; Park, S. J. *J. Solid State Electrochem.* **2012**,*16*,2751.
14. Zhou, X. H.; Li, L.F.; Dong, S. M. *J. Solid State Electrochem.* **2012**, *16*, 877.
15. Xiong, S.X.; Wei, J.; Jia, P.T.; Yang, L.P.; Ma, J.; Lu, X.H. *Appl. Mater. Interfaces* **2011**, *3*, 782.
16. Hyder, M. N.; Seung, W. L.; Cebeci, F. C. *Acs Nano* **2011**, *11*, 8552.
17. Zhao, L.; Fan, L. Z.; Zhou, M. Q.; Guan, H.; Qiao, S. Y.; Antonietti, M.; Titirici, M. M. *Adv. Mater.* **2010**,*22*,5202.
18. Shao, L.; Jeon, J. W. *Chem. Mater.* **2012**, *24*, 18.
19. Sun, X. F.; Xu, Y. L.; Wang, J. *J. Solid State Electrochem.* **2012**, *16*, 1781.
20. Biswas, S. J.; Lawrence, T. D. *Chem. Mater.* **2010**, *22*, 5667.
21. Graeme, M. S.; Colin, G. C.; Michael, S. F. *J. Electrochem. Soc.* **2010**, *157*, 1030.
22. Liu, D. Y.; Reynolds, J. R. *Appl. Mater. Interfaces* **2010**, *12*, 3586.
23. Fusalba, F.; Gouerec, P.; Villers, D.; Belanger, D. *J. Electrochem. Soc.* **2001**, *148*, A1.
24. Wang, K.; Huang, J. Y.; Wei, Z. X. *J. Phys. Chem. C* **2010**, *114*, 8062.
25. Zheng, L. P.; Wang, X. Y.; An, H. F.; Wang, X. Y; Yi, L. H.; Bai, L. *J. Solid State Electrochem.* **2011**, *15*, 675.
26. Pan, L. J.; Pu, L.; Shi, Y. *Adv. Funct. Mater.* **2006**, *16*, 1279.
27. Wu, J. H.; Tang, Q. W.; Li, Q. H. *Polymer* **2008**, *49*, 5262.
28. Keiser, H.; Beccu, K. D.; Gutjahr, M. A. *Electrochim. Acta* **1976**, *21*, 539.